Measurement 55 (2014) 394–401

Contents lists available at ScienceDirect

Measurement

journal homepage: www.elsevier.com/locate/measurement

# Aerosol laser time-of-flight mass spectrometer for the on-line measurement of secondary organic aerosol in smog chamber

Mingqiang Huang [a,b], Xingqiang Liu [b], Changjin Hu [c], Xiaoyong Guo [c], Xuejun Gu [c], Weixiong Zhao [c], Zhenya Wang [c], Li fang [c], Weijun Zhang [c,*]

[a] College of Chemistry & Environment, Minnan Normal University, Zhangzhou 363000, China
[b] Department of Environmental Science and Engineering, Xiamen University, Tan Kah Kee College, Zhangzhou 363105, China
[c] Laboratory of Atmospheric Physico-Chemistry, Anhui Institute of Optics and Fine Mechanics, Chinese Academy of Sciences, Hefei 230031, China

ARTICLE INFO

*Article history:*
Received 21 June 2013
Received in revised form 22 May 2014
Accepted 27 May 2014
Available online 7 June 2014

*Keywords:*
Toluene
Secondary organic aerosol (SOA)
Laser desorption/ionization
Aerosol laser time of flight mass spectrometer (ALTOFMS)
Appearance probability

ABSTRACT

An aerosol laser time of flight mass spectrometer (ALTOFMS) that can be used for real-time measurement of the size and composition of individual aerosol particles has been designed and utilized to provide on-line measurement of secondary organic aerosol (SOA) particles resulted from Cl-initiated oxidation of toluene in smog chamber. Both the size and chemical compositions of individual aerosol particles were obtained in real-time. According to a large number of single aerosol diameters and mass spectra, the size distribution and chemical composition of aerosol were determined statistically. Experimental results indicate that aerosol particles produced from Cl-initiated oxidation of toluene were predominantly in the form of PM 2.5 particles, and nine positive laser desorption/ionization mass spectra peaks: $m/z$ 18, 29, 30, 44, 46, 52, 65, 77, and 94 may come from the fragment ions of the products of the SOA: aromatic aldehydes, aromatic acids, phenolic compounds, and nitrogenated organic compounds. These results were in good agreement with those ones from previous Cl-initiated oxidation of toluene. These were demonstrated that ALTOFMS is a useful tool to reveal the formation and transformation processes of SOA particles in smog chamber.



## 1. Introduction

It is well-known that aromatic hydrocarbons such as benzene, toluene, ethylbenzene, xylenes, and trimethylbenzene contribute about 10% to the total global anthropogenic non-methane hydrocarbon (NMHC) emission [1,2], and toluene is the most abundant aromatic hydrocarbon among them [3,4]. Besides its carcinogenic and mutagenic effects on living organisms and human health [5], the degradation of toluene in the troposphere contributes substantially to the ozone and photooxidant burden and also the formation of secondary organic aerosol (SOA) [6–8], which are known to be harmful to human and ecosystem health [9–12]. Due to such environmental impacts atmospheric reactions of toluene has received much attention during the last few decades. The main oxidation and degradation way of toluene is assumed to be the reaction with OH radicals [6–8], but reactions with ozone, $NO_3$ and halogens also have significant contribution [13]. Cl atom high reactivity renders Cl-reaction as an efficient loss pathway for toluene particular in the marine boundary layer, polar and coastal areas where relatively high concentration of reactive halogens are observed [14–16]. Under a high chlorine regime, the degradation rate of volatile organic compounds (VOC) by Cl

* Corresponding author. Tel.: +86 551 65591551.
*E-mail address:* wjzhang@aiofm.ac.cn (W. Zhang).

http://dx.doi.org/10.1016/j.measurement.2014.05.038
0263-2241/

can dominate OH-initiated reactions due to up to two orders of magnitude faster reactions of Cl atom with VOC in comparison to OH radicals [17–21].

Over the past decade, the chemistry of SOA formation has been studied using smog chamber. Chemical composition of SOA particles was often studied by off-line techniques. The particles were usually collected using filters or impactor plate and samples were prepared by the way of chemical extracts. Molecular composition of SOA particles could be analyzed by Gas Chromatograph/mass spectrometer (GC–MS) [22–26], or Fourier transform infrared spectroscope (FTIR) [23]. However, the off-line techniques are time-consuming and tend to have sampling artifacts [27]. In addition, it is difficult to measured the size and chemical compositions of the individual SOA particles simultaneously and in real-time by using the off-line techniques. From the mid 1990s, a number of real-time single particle mass spectrometry techniques have been developed, offering new opportunities for on-line studying aerosol particulate matters [28,29]. Among these techniques, aerosol laser time-of-flight mass spectrometry (ALTOFMS) can be used to determine both the size and chemical composition of individual particles in real-time [29]. The application of ALTOFMS to the SOA particles was started in the 2001. Angelino et al. [30] used ALTOFMS to characterize the aerosol particles formed from reactions of secondary and tertiary alkylamine. On-line measurements of SOA particles formed from photooxidation of 1,3,5-tri methylbenzene, toluene and ethylbenzene using ALTOFMS was conducted by Gross et al. [31] and Wang et al. [32] and Huang et al. [33,34], respectively. However, unlike the conventional aerosol instruments, ALTOFMS can derive thousands of mass spectra during data acquisition in each experiment, which requires an efficient statistical method to classify these mass spectra according to their chemical composition.

We have recently developed an improved aerosol laser time of flight mass spectrometer (ALTOFMS) for real-time single-particle measurements. The ALTOFMS is capable of high time-resolution measurements of the size and chemical compositions of individual particles. Either the positive or negative-ion mass spectra are obtained for individual particles by changing the voltage polarity of the instrument. The ALTOFMS has a simple inlet and optical design, so that all particles detected by scattered light are virtually hit by desorption/ionization laser pulses. An improved data acquisition and processing system developed in our laboratory can be used to get the appearance probability of the certain mass spectra [32,33]. So according to a large number of single aerosol diameters and mass spectra, the size distribution and chemical composition of aerosol were determined statistically. In this paper, we present the results from chamber studied of SOA formation from Cl-initiated oxidation of toluene. Then the SOA chemical composition was analyzed by the on-line ALTOFMS with the aid of appearance probability processing system. Our motivation is to demonstrate whether the ALTOFMS coupled with appearance probability processing system is a useful tool to reveal the formation and transformation processes of SOA particles in smog chambers.

## 2. Experimental

### 2.1. Material

Benzaldehyde, phenol, benzoic acid, nitrobenzene, toluene, and 2-propanol (>99%) was obtained from Sigma–Aldrich Chemistry Corporation, Germany. Sodium nitrate (>99%) and methanol (>99%) were purchased from the Tianjin (The third Reagent Manufactory), nitrogen oxide and $Cl_2$ (99.9%) from Nanjing Special Gas Factory.

### 2.2. Generation of standard aerosol particles

The current knowledge of laser desorption/ionization (LDI) processes is still relatively limited. However, the typical features in the resulting mass spectra strongly depend on the operating conditions of the laser (i.e., wavelength, power, beam homogeneity). Moreover, when probing a particle with a high energy laser pulse, there is the possibility of rearrangements and/or reactions of the particle constituents in the laser plume. Therefore, understanding the complexity of ion formation processes, in particular when analyzing organic substances, requires detailed studies of the fragmentation patterns for the chemical class of interest under the same experimental conditions [30]. To this end, a preliminary investigation was carried out to characterize the behavior of benzaldehyde, phenol, benzoic acid, and nitrobenzene which are observed to be the major products formed from Cl-initiated oxidation of toluene [17–19]. Each compound was dissolved in 2-propanol (about $\sim 1 \times 10^{-5}$ g ml$^{-1}$) without further purification. Standard aerosol particles were generated from the solution by a constant output atomizer (TSI Inc. Model 3076), and subsequently passed through a diffusion dryer (TSI Inc. Model 3062) to decrease the humidity. All aerosol particles were passed through an $^{85}$Kr charge neutralizer (TSI Inc., Model 3054) before entering ALTOFMS. The typical initial concentrations of the standard particles were 10,000–50,000 particles cm$^{-3}$ with number mean diameter of 90–140 nm. The resulted dried aerosol particles were directly introduced to the ALTOFMS, and 1000 pieces of mass spectrum were got for each compound using for analyzing the appearance probability of mass spectra peaks.

### 2.3. Smog chamber experiments

Oxidation of toluene was performed using UV-irradiation of aromatic hydrocarbon/$Cl_2$/NO/air mixtures in our home-made smog chamber, the overall system components have been presented in detail previously [34,35] and will only be briefly described here. The experimental setup consists of a smog chamber and manifold system. The smog chamber is made of FEP-Teflon film, and its volume and the ratio of surface to volume are 1 m$^3$ and 6.5 m$^{-1}$ respectively. The reactor is surrounded by 12 fluorescent black lamps used to initiate the reactions. The output power of each black lamp is 20 W and its wavelength of UV radiation is 300–400 nm. The volume of glass

manifold system is 0.84 liter, equipped with a vacuum gauge whose measuring range is 10–5000 Pa.

Pure air system consists of an air compressor, drying system, particle filtering system, and zero air supply (TEI, model 111, USA). Pure air system produces pure air at rates up to 10 L/min at pressures of $1.72 \times 10^5$ Pa. The reactor of zero air supply, which is setted to 350 °C, removes hydrocarbons (HCs). The pure air has no detectable non-methane HCs (NMHC < 1 ppb), $NO_x$ (<1 ppb), has low $O_3$ concentration (<3 ppb), and low particle densities (<5 particles/$cm^3$), and relative humidity (RH) below 15%.

Prior to start each experiment, the chamber was continuously flushed with purified laboratory compressed air for 60 min. Toluene was sampled by a micro liter injector and injected directly into a small heated glass tube and dispersed into the chamber using the pure air flow. NO and $Cl_2$ were expanded into the evacuated manifold to the desired pressure through Teflon lines, and introduced into the smog chamber by a stream of pure air. And again the chamber was filled with the pure air to full volume. Then turn on four black lamps and initiate the photooxidation reaction. Chlorine atoms were generated by the photolysis of $Cl_2$ in air at wavelengths longer than 300 nm [17–21].

A series of experiments were carried out to investigate SOA from the Cl-initiated oxidation of aromatics under the conditions summarized in Table 1. And the SOA particles produced by the photooxidation were analyzed by the ALTOFMS connected directly to the chamber using a Teflon line.

### 2.4. Aerosol laser time-of-flight mass spectrometer (ALTOFMS)

Our ALTOFMS consists of sampling system of aerosol particle, sizing system of aerosol particle, timing circuit, linear time of flight mass spectrometer, a pulsed KrF excimer laser, data acquisition and processing system, and control software [32–34]. Two different kinds of time of flight techniques were employed in the ALTOFMS: one for measuring the size of the SOA particles, and the other for analyzing molecular composition of the same SOA particle. Aerosol particles produced in the smog chamber were introduced into the sizing system of the particles through a sampling system of ALTOFMS with an aerodynamic lens. In the sizing system of the particles, the particles passed through two continuous –wave laser beams with the detected scattering pulses sent to a timing circuit. The timing circuit could be used to measure the time of flight of the SOA particle and to track the same particle, whose diameter was measured just before. The timing circuit can read the time of flight required for the particle to pass the distance between the scattering laser beams, determine when each particle will be in the focal zone of an ablation laser, and prepare a pulsed KrF excimer laser very soon to perform laser desorption/ionization of a SOA particle at appropriate time based on the particle velocity which was calculated using the distance and the particle time-of-flight. An external size calibration uses particles of known size to relate the velocity to a physical aerodynamic diameter. The particle size calibration of ALTOFMS is determined by sampling diocyl phthalate (DOP) particles produced by TSI 3940 system (TSI Model 3940), which had been stored within a computer in advance. Once the laser has fired, the computer will read the data of the time of flight from the flight time data latch, acquire the signal of mass spectrum from the ion detector of a linear time of flight mass spectrometer, and send the master reset signal to prepare the timing circuit for the next track and the fire event.

In the experimental study on the photooxidation of aromatic hydrocarbons, the ALTOFMS was connected with our home-made smog chamber, and used to analyze the size, size distribution and molecular compositions of SOA particles produced from the photooxidation processes. The 248 nm laser beam from a pulsed KrF excimer laser intersected perpendicularly with the particle beam for desorption/ionization of them in the ion source. The ions produced here were mass-analyzed with a linear TOFMS mounted in a direction perpendicular to the plane defined by the molecular beam and laser photon beam. Then ions enter the flight tube (100 mm i.d. × 1000 mm), and the ion signal is detected by a dual microchannel plate detector (MCP) fixed at the end of the flight tube and sent to a pre-amplifier then recorded by a transient recorded interfaced to a personal computer. The pressure in the TOFMS chamber is $\sim 7.5 \times 10^{-5}$ Torr. By monitoring the ion current from the MCP as a function of time, a complete mass spectrum is obtained for the chemical compositions of a single particle. During the whole experiment, the pulse energy of the 248 nm laser is ~1–2 mJ with 20 ns pulse duration, which provides a power density of $\sim 1 \times 10^7$ - W $cm^{-2}$ when the laser spot size is 1 mm.

Each mass spectrum contains 4096 data points, corresponding to ion signal intensity. The particle mass spectra were calibrated using software which was compiled in Visual C++ developed by our laboratory. A list containing the area and exact mass-to-charge ratio of all peaks in each particle mass spectrum is generated. Peaks less than 10 arbitrary units above baseline on a 256-unit scale or with areas of less than 30 arbitrary units were rejected [32–34]. Each revised spectrum is then converted to a normalized 300-point vector, each point representing one mass unit. Then the positive ion mass spectra of a single particle are described as 300-dimensional data vectors using the ion masses as dimensions and the ion signal peak areas as values. Using the origin software, we can get not only the total number of mass spectra ($N_{tol}$) during each experimental study, but also the appearance frequency ($N_{af}$) of a mass spectra peak with a special ratio of mass to charge. The appearance probability ($A_p$) of a mass spectra peak

**Table 1**
Summary of the experimental conditions.

| Experiment No. | Aromatic | [Aromatic] (ppbv) | [$Cl_2$] (ppbv) | [NO] (ppbv) | 4 Black lamps |
|---|---|---|---|---|---|
| 1 | Toluene | 0 | 0 | 0 | On for 4 h |
| 2 | Toluene | 1000 | 0 | 0 | On for 4 h |
| 3 | Toluene | 0 | 0 | 500 | On for 4 h |
| 4 | Toluene | 0 | 2000 | 0 | On for 4 h |
| 5 | Toluene | 0 | 2000 | 500 | Off for 4 h |
| 6 | Toluene | 1000 | 2000 | 500 | On for 4 h |

can be defined as the ratio of its appearance frequency ($N_{af}$) to the total number ($N_{tol}$) of mass spectra ($A_p = N_{af}/N_{tol}$). For example, for the toluene photooxidation experiment, the total number of mass spectra ($N_{tol}$) is 1000, and the appearance frequency ($N_{af}$) of a mass spectra peak with a special $m/z$ 44 is 360, so the appearance probability of $m/z$ 44 mass spectra peak is 36%.

## 3. Results and discussion

### 3.1. Size distribution of SOA particles

The ALTOFMS instrument, sampling through the aerodynamic lens used here, is known to have size-dependent transmission of particles into the instrument. The transmission and detection for smaller particles is significantly less efficient than that for larger particles. And as described in the Experimental methods section, an external timing circuit sends a triggering pulse to fire the KrF laser when the sized particle arrives in the ion source region of the ALTOFMS. In general, not all particles that are sized produce mass spectra. As proposed by Allen et al. [36] detection efficiency of the particles $D_E$, is defined as the ratio between the number of particles hit by the LDI laser that generate ions detectable by the mass spectrometer and the total number of particles sampled into the ALTOFMS during the same time period. In this work, the number concentration of particles sampled into the ALTOFMS was measured using a commercially available scanning mobility particle sizer (SMPS;TSI 3080L DMA, TSI 3775 CPC). SMPS was chosen because of its ability to provide fast measurements, high resolution data, and wide concentration range from 1 to $10^7$ particles/cm$^3$. $D_E$ is calculated by the following equation:

$$D_E = N_H/C_{SMPS}Q$$

where $N_H$ is the number of particle hits per minute (particles/min); $C_{SMPS}$ is the particle number concentration measured by the SMPS (particles/cm$^3$), and $Q$ is the flow rate of the sampling inlet (cm$^3$/min). Particle detection efficiency is an important parameter for evaluating the performance of the ALTOFMS, This parameter depends on the performance of the sampling inlet and the components used for light scattering measurement, as well as on the particle size, shape, and chemical composition.

Fig. 1 shows the size distributions of the sized and hited particles as well as the variation of particle detection efficiency in Run 6. The current ALTOFMS has detection efficiencies ranging from ~25% to ~1% for aromatic SOA particles as a function of particle size. It is relatively uniform for aromatic SOA particles between 600 and 1,200 nm but decreased nearly to zero beyond this range. Aerosols created by these aromatics are predominate in the form of fine particles, which have diameter less than 2.5 μm (PM 2.5), Studies have shown that these fine particulate matters are more easily deposit in the lung of the human being, and do great harmful to the health [12].

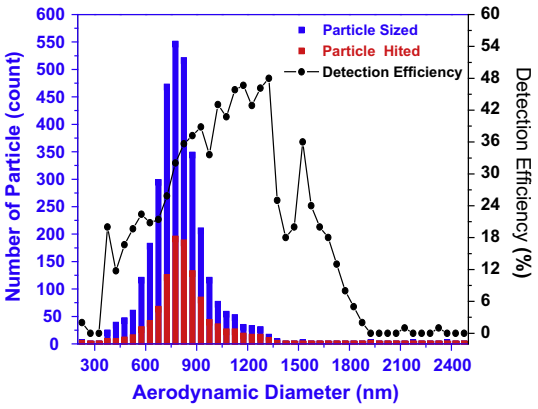


**Fig. 1.** Size distribution of the sized and hit particles as the variation of particle detection efficiency during Cl-initiated oxidation of toluene.

### 3.2. Laser desorption/ionization mass spectra of standard particles

The positive laser desorption/ionization mass spectra of standard particles measured by the ALTOFMS were obtained by averaging 50 spectra are shown in Fig. 2. As shown in Fig. 2(a), the mass spectra of benzaldehyde particles has the parent ions of $m/z$ 106. In general, the most important primary fragmentation process occurring for benzaldehyde involves the cleavage of the C–C bond, with loss of aldehyde group, leading to the formation of $m/z$ 29 ($HCO^+$) and benzene ion. Moreover, benzene ion in the high energy laser plume can crack to smaller fragments [37], such as the signals at $m/z$ 65$[C_5H_5]^+$, 52$[C_4H_4]^+$, 39$[C_3H_3]^+$, and 28$[C_2H_4]^+$. According to the results of the data acquisition and processing, appearance probability of major $m/z$ of standard aerosol particles are listed in Table 2. $m/z$ 29 has the highest appearance probability among all the mass peaks of benzaldehyde.

In addition to the signals at $m/z$ 77$[C_6H_5]^+$, 65$[C_5H_5]^+$, 52$[C_4H_4]^+$(Fig. 2(b)), ALTOFMS analysis of benzoic acid particles produces spectra with the most abundant signals at $m/z$ 44 accompanied by $m/z$ 18 which is similar to LDIMS of carboxylic acids obtained by Alfarra et al [38]. Mass fragment 44 has the appearance probability of 95% corresponds to the $CO_2^+$ fragment and laboratory experiments have shown that it arises, along with a mass fragment 18 ($H_2O^+$) which has the appearance probability of 91%, from decarboxylation of carboxylic acids [38].

In the LDI–MS of phenol particles shown in Fig. 2(c) with parent ions $m/z$ of 94, and fragments of benzene ion of $m/z$ 65$[C_5H_5]^+$, 52$[C_4H_4]^+$, 39$[C_3H_3]^+$, and 28$[C_2H_4]^+$. $m/z$ 94 has the appearance probability as high as 92%. This result indicates that phenolic compound in aerosol particles provide intense $m/z$ 94 in the positive mass spectra under our experimental conditions. In contrast, molecular ion was not found in the mass spectra of nitrobenzene particles. Besides the signals at $m/z$ 77$[C_6H_5]^+$, 65$[C_5H_5]^+$, and 52$[C_4H_4]^+$, two intensive signals were observed at $m/z$ 30 and 46 as shown in Fig. 2(d). Mass fragment 30 and 46 have the appearance probability of 92%, and 96%, and can be mostly interpreted as $NO^+$ and $NO_2^+$ from via cleavage

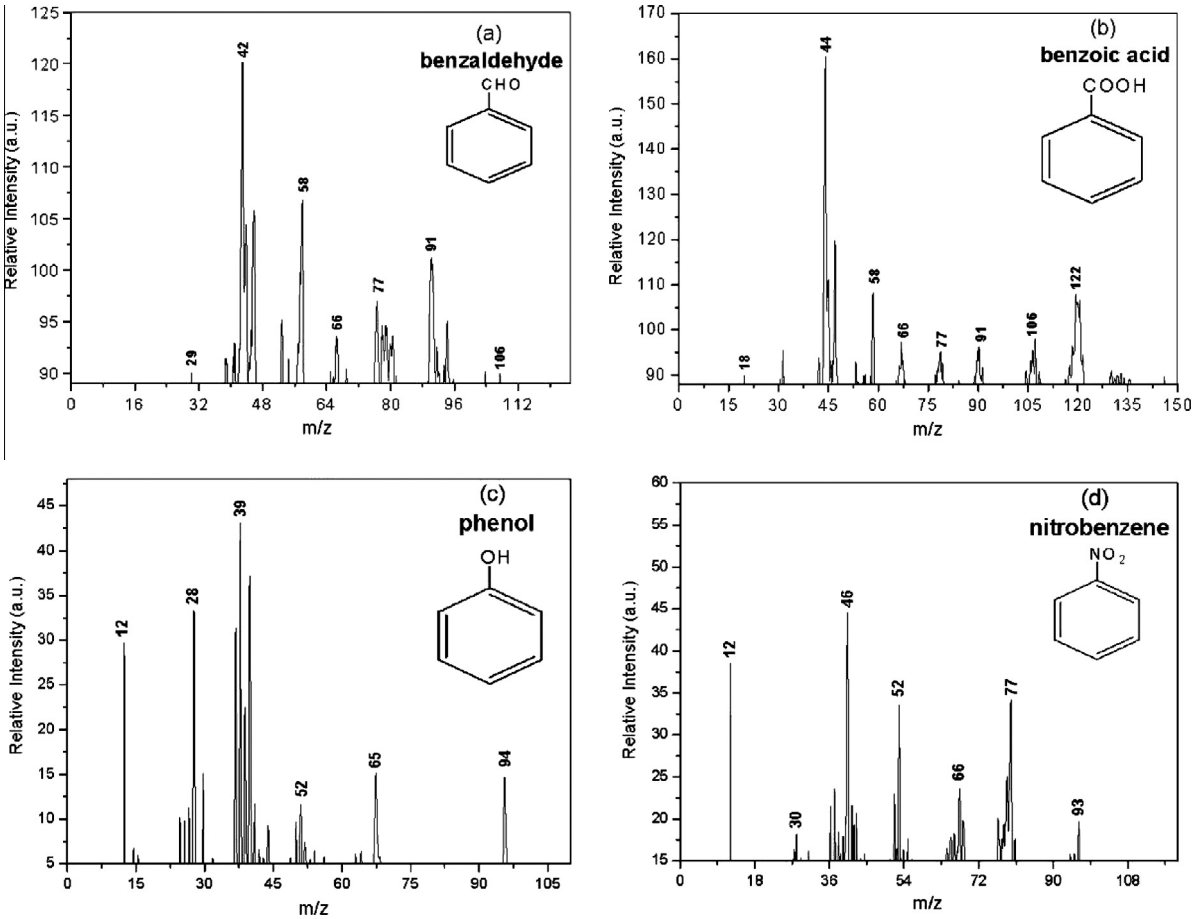


**Fig. 2.** Laser desorption/ionization time-of-flight mass spectra of (a) benzaldehyde ($M_w$ 106), (b) benzoic acid ($M_w$ 122), (c) phenol ($M_w$ 94), and (d) nitrobenzene ($M_w$ 123) particles.

**Table 2**
Appearance probability of *m*/*z* of standard aerosol particles and SOA from oxidation of toluene.

| *m*/*z* | 18 | 29 | 30 | 44 | 46 | 52 | 65 | 77 | 94 | 106 | 122 |
|---|---|---|---|---|---|---|---|---|---|---|---|
| Benzaldehyde | – | 93% | – | – | – | 66% | 73% | 85% | – | 76% | – |
| Benzoic acid | 91% | – | – | 95% | – | 61% | 69% | 78% | – | – | 72% |
| Phenol | – | – | – | – | – | 43% | 54% | 68% | 92% | – | – |
| Nitrobenzene | – | – | 92% | – | 96% | 55% | 67% | 79% | – | – | – |
| SOA | 58% | 91% | 42% | 65% | 45% | 39% | 47% | 62% | 53% | 28% | 25% |

of C–N bond. In fact, in previous LDI studies [38–40], a number of nitro-compounds have been shown to produce the ion peaks at *m*/*z* 30 and 46.

### 3.3. Laser desorption/ionization mass spectra of SOA particles in smog chamber

According to the design principles on the measuring system of particle diameter, timing circuit, and laser desorption/ionization setup of ALTOFMS, its time of flight mass spectroscopy is only obtained from those particles of secondary organic aerosol, whose diameter has been measured. The diameter of individual particle, number distribution of SOA particle diameter, and molecular composition of SOA particle could be measured using our ALTOFMS. 5468 pieces of mass spectrum were got for run 6 after 1 h oxidation. Fig. 3 shows the size and laser desorption/ionization time-of-flight mass spectra and of 4 individual SOA particles. It is told that each piece of mass spectrum corresponds to an aerosol particle, and the diameter and chemical composition might be different from each other. Under typical LDI conditions, ALTOFMS mass spectra often do not allow for definitive identification of the organic compounds present in the condensed phase. However, the observed signals may serve as useful indicators for some of the major constituents and thus the reaction mechanism leading to particle formation. As shown in Fig. 3, the mass spectra of SOA particles typically exhibit

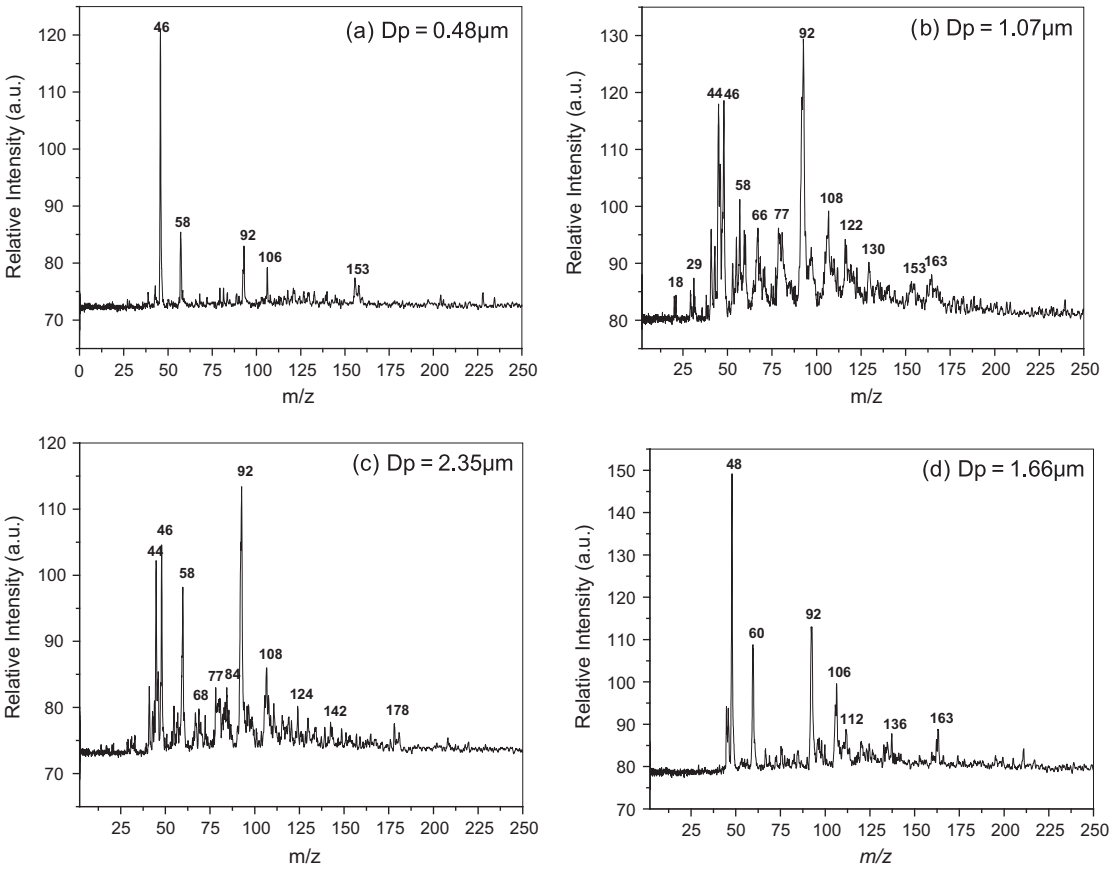


**Fig. 3.** Laser desorption/ionization time-of-flight mass spectra and size of 4 individual toluene SOA particles after 4 h photooxidation. Aerosol diameter (a) 0.48 μm; (b) 1.07 μm; (c) 2.35 μm and (d) 1.66 μm.

similar features of standard particles in the low mass range, indicating that analogous fragmentation patterns for most of the compounds formed in the Cl-initiated oxidation of toluene and standard aerosol particles of benzaldehyde, phenol, benzoic acid, and nitrobenzene.

Mass fragment 29 has the highest appearance probability among all the mass peaks of SOA particles shown in Table 2. It may arise from short carbon chain $C_2H_5^+$, or from carbonyl- containing compounds[36], such as aromatic aldehyde, in the form of $HCO^+$, which is more likely to be the case in this study. Benzaldehyde is possible candidate compound to be ionized to produce *m*/*z* 29. As proposed by Atkinson et al [13], the Cl-initiated reaction results in major hydrogen abstraction from methyl group to form a benzyl radical. As shown in Fig. 4, benzyl radical reacts with $O_2$ to form benzyl peroxy radical, which can undergo self-reaction to form benzaldehyde, or react with NO to form an alkoxy radical and $NO_2$. Oxygen can abstract a hydrogen atom from the alkoxy radical to form benzaldehyde. The appearance probability of *m*/*z* 29 is as high as 91%, showing a very good agreement with the experimental results of Wang et al [18].

The mass spectra of SOA particles are characterized by a very intense mass fragment at *m*/*z* 44 correspond to $CO_2^+$ along with mass fragments at *m*/*z* 18 ($H_2O^+$) and *m*/*z* 77($C_6H_5^+$), showing that the particles produced from Cl-initiated oxidation of toluene contain aromatic organic acids. It is in good agreement with previous reaction studies, where highly oxidized chemical classes from Cl-initiated oxidation of toluene like benzoic acid had been reported under different concentration [17]. Cl abstracts a hydrogen atom from the carbonyl group of benzaldehyde, and oxygen adds to the radical. This peroxy radical can react with $RO_2$ (or $HO_2$) to form the benzoic acid directly, or it can react with NO to form an alkoxy radical and $NO_2$. The alkoxy radical can abstract a hydrogen from another toluene molecule, or from a benzaldehyde molecule, to yield the benzoic acid and to propagate the radical chain reaction. Fig. 4 also outlines this suggested mechanism leading to the benzoic acid.

Mass fragment 30 and 46 are interpreted as $NO^+$ and $NO_2^+$. Their appearance may imply the formation of nitrogenated organic compounds from Cl-initiated oxidation of toluene in the presence $NO_x$. Some experimental studies have examined and reported the formation of nitrogenated organic compounds from oxidation of toluene and other aromatic compounds [22–26]. The contribution of alkyl nitrates ($RONO_2$) and peroxyacyl nitrates ($RC(O)OONO_2$) to the secondary organic aerosol formation was positively verified using FTIR spectroscopy [23]. Similar to the

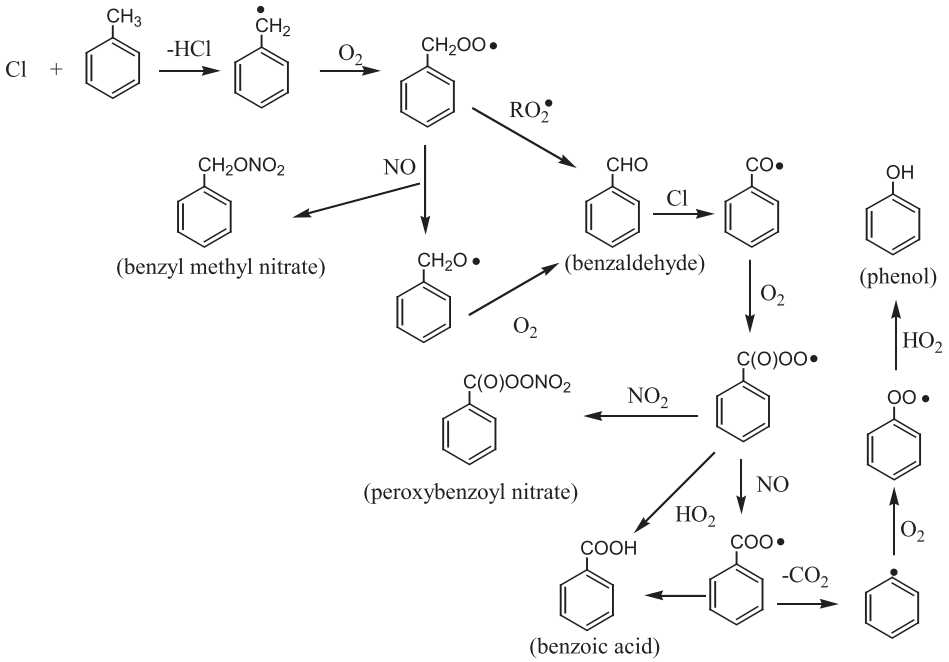


**Fig. 4.** Proposed reaction mechanism for Cl-initiated oxidation of toluene.

OH-initiated oxidation of toluene, the resulting benzyl peroxy radical may react with NO to form benzyl methyl nitrate. In addition, following the H-atom abstraction process of benzaldehyde by Cl atoms, $O_2$ rapidly adds to the radical to form peroxy radical which can react with $NO_2$ to form peroxybenzoxyl nitrate, which was shown in Fig. 4.

Mass fragment 77, 65, and 52 are the signature of $C_6H_5^+$ and its fragment ion $C_4H_4^+$and $C_3H_3^+$. They may come from the particles produced from the Cl-initiated oxidation of toluene contained aromatic ring retaining products, which has already been reported in many chamber studies [17–19]. These observed aromatic ring retaining products might be the aromatic aldehydes, aromatic acids, and nitrogenated organic compounds discussion mentioned above.

*m*/*z* 94 fragment may proposed as $C_6H_5OH^+$. It is shown that the particles produced from Cl-initiated oxidation of toluene may contain phenolic compounds species. Cai et al. [17] has detected and identified phenol resulting from Cl-initiated oxidation of toluene in the presence $NO_x$. As shown in Fig. 4, the resulting alkoxy radical from benzaldehyde react with Cl atom, $O_2$, and NO can crack to form $CO_2$ and phenyl radical, which can further react with $O_2$ to form phenyl peroxy radical which can react with $RO_2$ (or $HO_2$) to form the phenol directly.

From our experimental results and discussion mentioned above, it is shown that, nine positive laser desorption/ionization mass spectra peaks: *m*/*z* 18, 29, 30, 44, 46, 52, 65, 77, and 94 may come from the fragment ions of the products of the SOA: aromatic aldehydes, aromatic acids, phenolic compounds, and nitrogenated organic compounds. These results show a good agreement with the previous aromatic hydrocarbons smog chamber experiments [17–19]. Different from AMS [36], we can obtain the size and chemical composition of individual SOA particles in real-time, according to a large number of single SOA particles mass spectra, the chemical compositions of SOA were got statistically. These were demonstrated that ALTOFMS is a useful tool to reveal the formation and transformation processes of SOA particles in smog chamber.

## 4. Conclusion

In this paper, we have demonstrated that aerosol laser time-of-flight mass spectrometer (ALTOFMS) can be used to measure secondary organic aerosol form from Cl-initiated oxidation of toluene in real-time. We showed that SOA mass spectra have nine positive laser desorption/ionization mass spectra peaks: *m*/*z* 18, 29, 30, 44, 46, 52, 65, 77, and 94 may come from the fragment ions of the products of the SOA: aromatic aldehydes, aromatic acids, phenolic compounds, and nitrogenated organic compounds. We have demonstrated that ALTOFMS can be used to investigate the formation and transformation processes of SOA particles in smog chambers.

## Acknowledgements

This work is supported by National Natural Science Foundation of China (No. 41305109), Natural Science Foundation of Fujian Province of China (No. 2012J05079) and the program for New Century Excellent Talents of Minnan Normal University (No. MX13001). Also, the authors express our gratitude to the referees for their valuable comments.

## References


[1] Y.J. Zhang, Y.J. Mu, P. Liang, Z. Xu, J.F. Liu, H.X. Zhang, X.K. Wang, J. Gao, S.L. Wang, F.H. Chai, A. Mellouki, Atmospheric BTEX and carbonyls during summer seasons of 2008–2010 in Beijing, Atmos. Environ. 59 (2012) 186–191.

[2] H.J. Avens, K.M. Unice, J. Sahmel, S.A. Gross, J.J. Keenan, D.J. Paustenbach, Analysis and modeling of airborne BTEX concentrations from the Deepwater Horizon Oil Spill, Environ. Sci. Technol. 45 (2011) 7372–7379.

[3] B.W. Wu, J.M. Hao, H. Takekawa, J.H. Li, K. Wang, J.K. Jiang, The remarkable effect of $FeSO_4$ seed aerosols on secondary organic aerosol formation from photooxidation of α-pinene/$NO_x$ and toluene/$NO_x$, Atmos. Environ. 55 (2012) 26–34.

[4] K. Kawamura, M. Vestergaard, M. Ishiyama, N. Nagatani, T. Hashiba, E. Tamiya, Development of a novel hand-held toluene gas sensor: possible use in the prevention and control of sick building syndrome, Measurement 39 (2006) 490–496.

[5] E. Durmusoglu, F. Taspinar, A. Karademir, Health risk assessment of BTEX emissions in the landfill environment, J. Hazard. Mater. 176 (2010) 870–877.

[6] Y. Zhou, H.F. Zhang, H.M. Parikh, E.H. Chen, W. Rattanavaraha, E.P. Rosen, W.X. Wang, R.M. Kamens, Secondary organic aerosol formation from xylenes and mixtures of toluene and xylenes in an atmospheric urban hydrocarbon mixture: water and particle seed effects (II), Atmos. Environ. 45 (2011) 3882–3890.

[7] J.H. Kroll, J.H. Seinfeld, Chemistry of secondary organic aerosol: formation and evolution of low-volatility organics in the atmosphere, Atmos. Environ. 42 (2008) 3593–3624.

[8] J.R. Odum, T.P.W. Jungkamp, R.J. Griffin, R.C. Flagan, J.H. Seinfeld, The aerosol-forming potential of whole gasoline vapor, Science 276 (1997) 96–99.

[9] Z. Wang, T. Wang, J. Guo, R. Gao, L.K. Xue, J.M. Zhang, Y. Zhou, X.H. Zhou, Q.Z. Zhang, W.X. Wang, Formation of secondary organic carbon and cloud impact on carbonaceous aerosols at Mount Tai, North China, Atmos. Environ. 46 (2012) 516–527.

[10] N.K. Kim, Y.P. Kim, C.H. Kang, Long-term trend of aerosol composition and direct radiative forcing due to aerosols over Gosan: TSP, PM10, and PM2.5 data between 1992 and 2008, Atmos. Environ. 45 (2011) (1992) 6107–6115.

[11] U. Baltensperger, Aerosols in clearer focus, Science 329 (2010) 1474–1475.

[12] A.E. Russell, B. Brunekreef, A focus on particulate matter and health, Environ. Sci. Technol. 43 (2009) 4620–4625.

[13] R. Atkinson, J. Arey, Atmospheric degradation of volatile organic compounds, Chem. Rev. 103 (2003) 4605–4638.

[14] J.P. Kercher, T.P. Riede, I.J.A. Thorton, Chlorine activation by $N_2O_5$: simultaneous, in situ detection of $ClNO_2$ and $N_2O_5$ by chemical ionization mass spectrometry, Atmos. Measur. Technol. 2 (2009) 193–204.

[15] K.W. Oum, M.J. Lakin, D.O. Dehaan, T. Brauers, B.J. Finlayson-Pitts, Formation of molecular chlorine from the photolysis of ozone and aqueous sea-salt particles, Science 279 (1998) 74–76.

[16] C.W. Spicer, E.G. Chapman, B.J. Finlayson-Pitts, R.A. Plastridge, J.M. Hubbe, J.D. Fast, C.M. Berkowitz, Unexpectedly high concentrations of molecular chlorine in coastal air, Nature 394 (1998) 353–356.

[17] X.Y. Cai, L.D. Ziemba, R.J. Griffin, Secondary aerosol formation from the oxidation of toluene by chlorine atoms, Atmos. Environ. 42 (2008) 7348–7359.

[18] L. Wang, J. Arey, R. Atkinson, Reactions of chlorine atoms with a series of aromatic hydrocarbons, Environ. Sci. Technol. 39 (2005) 5302–5310.

[19] R.S. Karlsson, J. SzenteJ, J.C. Ball, M.M. Maricq, Homogeneous aerosol formation by the chlorine atom initiated oxidation of toluene, J. Phys. Chem. A 105 (2001) 82–96.

[20] J.C. Shi, M.J. Bernhard, Kinetic studies of Cl-atom reactions with selected aromatic compounds using the photochemical reactor-FTIR spectroscopy technique, Int. J. Chem. Kinet. 29 (1997) 349–358.

[21] R. Atkinson, S.M. Aschmann, Kinetics of the gas-phase reactions of Cl atoms with a series of organics at 296 ± 2 K and atmospheric pressure, Int. J. Chem. Kinet. 17 (1985) 33–41.

[22] T.E. Kleindienst, T.S. Conver, C.D. McIver, E.O. Edney, Determination of secondary organic aerosol products from the photooxidation of toluene and their implications in ambient PM2.5, J. Atmos. Chem. 47 (2004) 79–100.

[23] M. Jang, R.M. Kamens, Characterization of secondary aerosol from the photooxidation of toluene in the presence of $NO_x$ and 1-propene, Environ. Sci. Technol. 35 (2001) 3626–3639.

[24] D.F. Smith, C.D. McIver, T.E. Kleindienst, Primary product distribution from the reaction of hydroxyl radicals with toluene at ppb $NO_x$ mixing ratios, J. Atmos. Chem. 30 (1998) 209–228.

[25] H.J.L. Forstner, R.C. Flagan, J.H. Seinfeld, Secondary organic aerosol from the photo- oxidation of aromatic hydrocarbon: molecular composition, Environ. Sci. Technol. 31 (1997) 1345–1358.

[26] J. Yu, H.E. Jeffries, K.G. Sexton, Atmospheric photooxidation of alkylbenzenes-I, carbonyl product analyses, Atmos. Environ. 31 (1997) 2261–2280.

[27] B.J. Turpin, P. Saxena, E. Andrews, Measuring and simulating particulate organics in the atmosphere: problems and prospects, Atmos. Environ. 34 (2000) 2983–3013.

[28] G. Buonanno, M. Dell'Isola, L. Stabile, A. Viola, Critical aspects of the uncertainty budget in the gravimetric PM measurements, Measurement 44 (2011) 139–147.

[29] K.A. Pratt, K.A. Prather, Mass spectrometry of atmospheric aerosols-recent developments and applications. Part II: On-line mass spectrometry techniques, Mass Spectrom. Rev. 31 (2011) 1–16.

[30] S. Angelino, D.T. Suess, K.A. Prather, Formation of aerosol particles from reactions of secondary and tertiary alkylamines: characterization by aerosol time-of-flight mass spectrometry, Environ. Sci. Technol. 35 (2001) 3130–3138.

[31] D.S. Gross, M.E. Gälli, M. Kalberer, A.S.H. Prevot, J. Dommen, M.R. Alfarra, J. Duplissy, K. Gaeggeler, A. Gascho, A. Metzger, U. Baltensperger, Real-Time measurement of oligometric species in secondary organic aerosol with the aerosol time-of-flight mass spectrometer, Anal. Chem. 78 (2006) 2130–2137.

[32] Z.Y. Wang, L.Q. Hao, L.Z. Zhou, X.Y. Guo, W.W. Zhao, L. Fang, W.J. Zhang, Real-time detection of individual secondary organic aerosol particle from photooxidation of toluene using aerosol time-of-flight mass spectrometer, Sci. China, Ser. B: Chem. 49 (2006) 267–272.

[33] M.Q. Huang, W.J. Zhang, L.Q. Hao, Z.Y. Wang, W.W. Zhao, X.J. Gu, X.Y. Guo, X.Y. Liu, B. Long, L. Fang, Laser desorption/ionization mass spectrometric study of secondary organic aerosol formed from the photooxidation of aromatics, J. Atmos. Chem. 58 (2007) 237–252.

[34] M.Q. Huang, L.Q. Hao, X.Y. Guo, C.J. Hu, X.J. Gu, W.X. Zhao, Z.Y. Wang, L. Fang, W.J. Zhang, Characterization of secondary organic aerosol particles using aerosol laser time-of-flight mass spectrometer coupled with FCM clustering algorithm, Atmos. Environ. 64 (2013) 85–94.

[35] G. Pan, C.J. Hu, Z.Y. Wang, Y. Cheng, X.H. Zheng, X.J. Gu, W.X. Zhao, W.J. Zhang, J. Chen, F.Y. Liu, X.B. Shan, L.S. Sheng, Direct detection of isoprene photooxidation products by using synchrotron radiation photoionization mass spectrometry, Rapid Commun. Mass Spectrom. 26 (2012) 189–194.

[36] J. Allen, D. Fergenson, E. Gard, L. Hughes, B. Morrical, M. Kleeman, D. Gross, M. Gälli, K. Prather, G. Cass, Particle detection efficiencies of aerosol time of flight mass spectrometers under ambient sampling conditions, Environ. Sci. Technol. 34 (2000) 211–217.

[37] P.J. Silva, K.A. Prather, Interpretation of mass spectra from organic compounds in aerosol time-of-flight mass spectrometry, Anal. Chem. 72 (2002) 3553–3562.

[38] M.R. Alfarra, D. Paulsen, M. Gysel, A.A. Garforth, J. Dommen, A.S.H. Prévôt, D.R. Worsnop, U. Baltensperger, H. Coe, A Mass spectrometric study of secondary organic aerosols formed from the photooxidation of anthropogenic and biogenic precursors in a reaction chamber, Atmos. Chem. Phys. 6 (2006) 5279–5293.

[39] A.W. Rollins, A. Kiendler-Scharr, J.L. Fry, T. Brauers, S.S. Brown, H.P. Dorn, W.P. Dubé, H. Fuchs, A. Mensah, T.F. Mentel, F. Rohrer, R. Tillmann, R. Wegener, P.J. Wooldridge, R.C. Cohen, Isoprene oxidation by nitrate radical: alkyl nitrate and secondary organic aerosol yields, Atmos. Chem. Phys. 9 (2009) 6685–6703.

[40] K. Sato, A. Takami, T. Isozaki, T. Hikida, A. Shimono, T. Imamura, Mass spectrometric study of secondary organic aerosol formed from the photo-oxidation of aromatic hydrocarbons, Atmos. Environ. 44 (2010) 1080–1087.